Journal of Solid Mechanics and Materials Engineering

Vol. 1, No. 1, 2007

Comparative Study of Nose Profile Role in Long-Rod Penetration*

Kamran DANESHJOU**, Majid SHAHRAVI**, Mohamad RAHIMZADEH**

** Department of Mechanical Engineering, Iran University of Science and Technology, Tehran, Iran
E-mail: kdaneshjo@iust.ac.ir

Abstract

In this paper the penetration depth of long-rod electromagnetic projectiles on semi-infinite targets are studied with numerical approach. And the role of nose profile was studied. The results obtained from this investigation were compared with the recent studies. For the targets and projectile were considered to be made of soft metals. All the results were compared with two analytical models: Tate and Vahedi. These two models don't consider the role of nose profile. The target is constrained to have no movement and the projectile doesn't pass through the target. The impact velocity of the projectile was considered as a variable and the results were compared together and they were in good agreement with other studies in this field.

***Keywords*:** Long-Rod, Nose Shape, Penetration, Semi-Infinite

1. Introduction

It has been long known that nose shape has a dramatic influence on the ability of non deforming projectiles to penetrate into targets[7,8&9]. Mullin et al. [7] performed experiments to measure the residual velocity of conical and blunt nose projectiles after perforation of steel plates. They found that the residual velocities of the conical nose projectiles were less massive (the projectiles had the same length and diameter, but the conical-nose projectile weight has because of the material removed to achieve a conical nose). In several of the experiments the blunt-nose projectiles failed to perforate the target whereas the conical-nose projectile perforated with more than a third of the original impact velocity. However in cases where the target was sufficiently hard to cause significant projectile erosion, the conical-nose projectiles did not perform as well as the blunt-nose projectiles. Batra [10] numerically investigated the effect of ellipsoidal nose shapes on steady-state penetration by a nodeforming projectile. By varying the ratio of the major to minor axes of the ellipsoidal nose, he was able to examine differences in penetration by a blunt-hemispherical, and an ellipsoidal-nose projectile. Batra found that the nose shape significantly affects the deformations of the target material in vicinity of the projectile/target interface. And that the axial resisting forces are considerably higher for the blunt-nose projectiles compared to the ellipsoidal nose projectile.

Walker and Anderson [1] examined numerically the role of the initial nose shape on the penetration capability of eroding long-rods. They found that after penetrating about two rod diameters, all the rods attained the same shape for the deformed nose profile with no resemblance to the initial nose shape. In addition they found that the largest differences in

*Received 2 Oct., 2006 (No. 06-0119)
[DOI: 10.1299/jmmp.1.x]

early time behavior were the high pressures the blunt-nose projectile delivered to the target and itself and subsequent effects due to these high pressures.

They also realized that the final penetration at the end of transient state (prior to steady state), for the three specific projectiles differs up to %3. The purpose of the work presented here was to further expand on these issues. Particularly, we investigated the role of deformed nose profile on the penetration capability of the long-rod. In addition there are comparisons done between these numerical results and Vahedi and Tate theoretical models.

2. Study of long-rod projectile penetration models in semi-infinite targets

A. Tate Model

In Tate & Alekseevskii penetration models [5, 11], the projectiles dynamics resistance is added to Bernoulli equation:

$$Y+\frac{1}{2}\rho_p(v-u)^2=\frac{1}{2}\rho_t u^2+R' \tag{1}$$

$$v=u-\dot{\ell} \tag{2}$$

$$u=\dot{P} \tag{3}$$

This modified Bernoulli equation is valid not only for the impact velocity v_p but also for any instantaneous rod velocity v and instantaneous penetration velocity u.

In these models a relation between the instantaneous rod length ℓ and instantaneous rod velocity v as a function of R',Y,v_p,ρ_p,ρ_t is developed. The relative magnitudes of Y,R' affects the penetration depth and cause three different cases. Considering the penetration depth equation:

$$P=\int_0^{T_0} u\,dt \tag{4}$$

Newton's law and also ignoring plastic wave propagation, the following relation for penetration depth is obtained:

$$\frac{P}{L}=f(v_p,\rho_p,\rho_t,R',Y) \tag{5}$$

B. Vahedi Model

In this model all velocity ranges from low velocity to hypervelocity are analyzed. This model is based upon the Assumptions of the steady-state penetration process, and is used in comparison with experimental measurements. In fact the most important advantage of this model is its simpleness and direct application in the design process. This model suggests quick results with sufficient accuracy for many applications.

The parametric study of penetration depth can be easily done using this model. These parameters include density, aspect ratio (L/D), yield strength, and the hydrodynamic velocity of both the target and projectile.

According to this parametric study, in low velocities all the parameters are of significant importance where as in hypervelocity, some of these parameters such as aspect ratio and strength can be ignored. The assumptions to obtain the formulation in this model are as follows [6]:

1. The transient penetration phase is neglected at the beginning of penetration.
2. The secondary phase (in which the penetration depth changes after the consumption of rod due the inertia of the impact between the target and the rod), is neglected.
3. The recovery is also neglected which means the penetration depth in the final phase is not reduced.
4. It is assumed that the erosion rate of projectile (the rate of the change in the length of the projectile) is proportional to the rod velocity.

5. The target resistance to penetration is a variable which depends on the impact velocity, target strength and the projectile's diameter and length.
6. It is assumed that the interaction between the target and projectile is considered one dimensional in the penetration process.
7. Heat transfer is neglected.

In the penetration process the rod length is divided into two parts: rigid and plastic (Fig.1). If the length of the unreformed part of the rod is denoted by ℓ at each moment, then:

$$M = \rho_p \ell A \tag{6}$$

$$\dot{\ell} = -\dot{x} \tag{7}$$

For the undeformed part of the rod the following equation which indicates the impact within the time interval Δt holds (Fig.2):

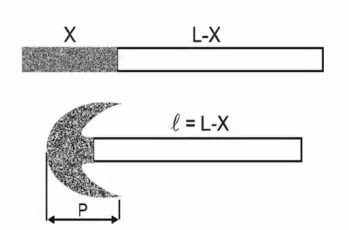

Fig.1. Long-Rod Scheme in Penetration Process

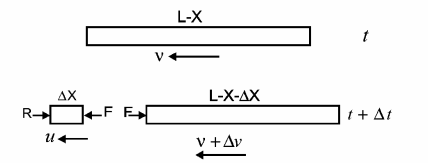

Fig.2. Mass Transfer from Undeformed into the Plastic Part

$$Momentom_{t+\Delta t} - Momentom_t = R\Delta t \tag{8}$$

Where R is the external force on the rod. Equation (8) can be rewritten as follows:

$$[(M + dM)(v + dv) - u\,dM] - Mv = Rdt \tag{9}$$

Substituting (6) into (9) and using (7) and (2), (10) can be obtained:

$$\rho_p A[\ell \frac{dv}{dt} - (v-u)^2] = R \tag{10}$$

Considering $p_0 = R/A$ the result is [6]:

$$\frac{dv}{dt} = \frac{(v-u)^2}{\ell} + \frac{p_0}{\rho_p \ell} \tag{11}$$

Model deals with 3 equation and 5 unknowns: equations (2), (3) & (10). Where the 5 unknowns are u, v, ℓ, p_0 *and* P.

There are some methods to obtain the two remaining equation, such as using Bernoulli equation or experimental relations. These methods have modified and have proved to be useful for engineering applications. The model's properties are:

1. This is a general model in which material type has not been specified and therefore can be used for all different materials.
2. Since no definite range has been considered, this model can be used for all velocity ranges.
3. In this model the aspect ratio (L/D) as been taken in to consideration; therefore it can be used for a wide range of L/D values.
4. The equations in this model are considerably simple and can be used for design problems.

5. This model enables us to study penetration parametrically.

3. Numerical analysis

A full three-dimensional explicit finite element analysis was carried out to investigate the semi-infinite problem. A general-purpose explicit finite element analysis code was used for the numerical calculations.

Figure 3 shows a typical finite element model used in the numerical analysis. The model consists of a cubic semi-infinite target and a cylindrically shaped projectile that is initially located 1 mm away from the target.

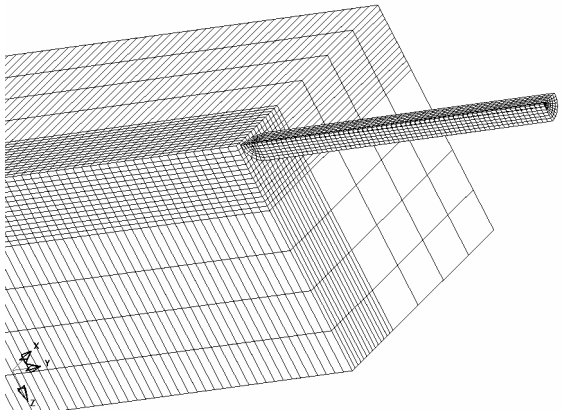

Fig.3. Typical Finite Element Mesh Coordinate System Used for the Numerical Study

Four nose profile assumed for the projectile: conical, hemispherical, blunt and T shaped (Fig.4).

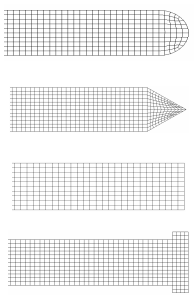

Fig.4. Schematic of Four Nose Shape is used in this Study

Only $1/4$ of the whole geometry was modeled due to the inherent symmetry of the model along the x and z-direction of the coordinate as shown in figure3. The length and diameter of the projectiles chosen for the numerical analysis were 74.7 and 7.1 mm, respectively given an L/D ratio of 10.5.

Impact velocities of the projectiles were varied from 300 to 1800 m/s with an increment of 300 m/s. target modeled are 40cm long, and 15×15 cm square cross section. Typical eight-node linear brick elements were used for meshing as shown in figure 3. Material properties were applied to the model by assigning appropriate material properties to the predefined projectiles and target elements sets, i.e. properties of steel to the projectile element set and properties of Aluminum, to the target element set.

In order to model a high strain-rate mechanical response of the projectile and the target materials, a commonly used constitutive equation, the Johnson-Cook equation, was used as it is known to describe high-velocity mechanical response of a number of metals fairly well. This has the form:

$$\sigma = (\sigma_0 + B\varepsilon_p^n)(1 + C\ln\frac{\dot{\varepsilon}}{\dot{\varepsilon}_0})[1 - (\frac{T - T_r}{T_m - T_r})^m] \quad (12)$$

Where σ_0 is the static yield strength, ε_p the effective plastic strain rate, T the temperature, T_r the room temperature, T_m the melting temperature and B, C, m and n are material constants. For the material used in this study, these parameters were taken from Johnson and Cook and are shown in table 1.

TABLE 1
Material Properties and Constants for the Johnson-Cook Model Applied to the Numerical Model

	σ_0 MPa	T_m K	B MPa	n	C	m
Target	265	775	426	0.34	0.015	1.00
Projectile	792	1793	510	0.26	0.014	1.03

4. Results and discussion

The analysis has been carried out for the model with four nose shape. The results have been compared with theoretical models. Figure 5 shows the comparison between Tate, Vahedi and Numerical model with the Blunt nose-shape projectile. The results illustrate the point that Vahedi model shows closer agreement with the numerical ones in comparison with Tate model. As depicted in figure 5, at impact velocity of 1200 m/s, the P/L obtained from Tate model is 0.92 while Vahedi and numerical model result respectively in 0.552, 0.534. This difference is due to taking L/D effect into account in Vahedi model which is one of effective parameters in penetration depth.

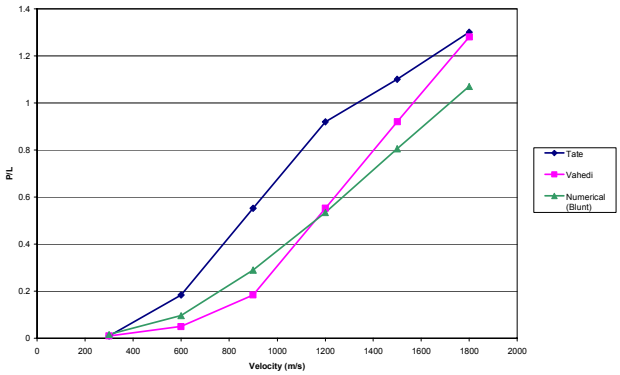

Fig.5. Comparison study of Tate and Vahedi to Numerical model with Blunt nose-shape

Figure 6 present a comparison between four different nose-shaped projectiles

(Hemispherical, Conical, Blunt and T shaped) based on the numerical model. again at impact velocity of 1200 m/s, the P/L for hemispherical, conical, blunt and T nose shaped projectiles obtained respectively, 0.621, 0.576, 0.534 and 0.460.

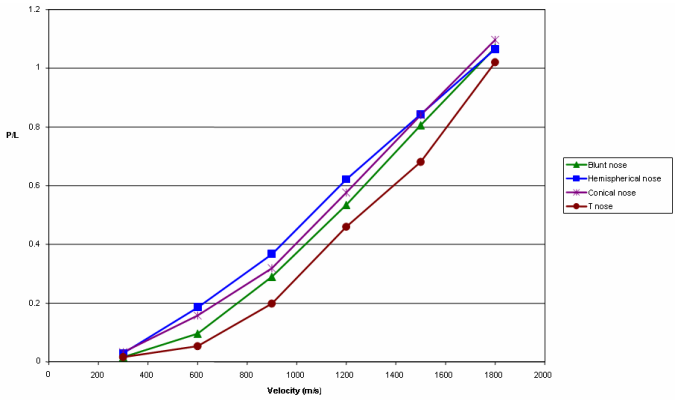

Fig.6. Comparison study of nose shape effect with numerical approach

As readily seen, the P/L of T shaped projectile is more different from the others. Table 2 and 3 present penetration depth and kinetic energy of different nose shaped projectile chronologically. According to these tables, figures 7 to 10 shows the penetration steps of four different nose shapes respectively in times 10, 40, 70 & 100 μs.

TABLE 2
Penetration Depth and Kinetic Energy of Blunt and Hemispherical nose-Shaped Projectile Chronologically

	Blunt nose-shape		Hemispherical nose-shape	
Time (μs)	Penetration (cm)	Kinetic energy(KJ)	Penetration (cm)	Kinetic energy(KJ)
0	0	4.12	0	4.12
10	0.7	3.72	0.67	3.79
40	2.27	2.52	2.26	2.57
70	3.42	1.53	3.59	1.56
100	3.97	0.4	4.42	0.88

TABLE 3
Penetration Depth and Kinetic Energy of Conical and T nose-Shaped Projectile Chronologically

	Conical nose-shape		T nose-shape	
Time (μs)	Penetration (cm)	Kinetic energy (KJ)	Penetration (cm)	Kinetic energy (KJ)
0	0	4.12	0	4.12
10	0.62	3.83	0.77	3.40
40	2.23	2.64	2.2	2.59
70	3.42	1.16	3.12	1.32
100	4.24	0.04	3.43	0.94

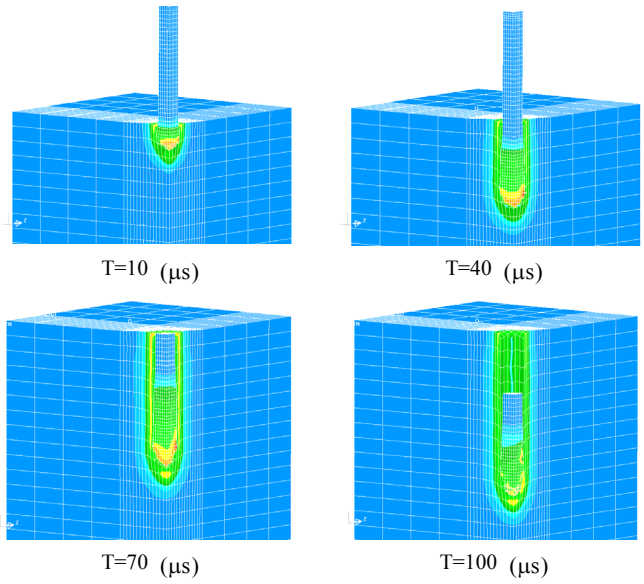

Fig.7. Penetration of Hemispherical Nose-Shape Projectile into the Target Chronologically

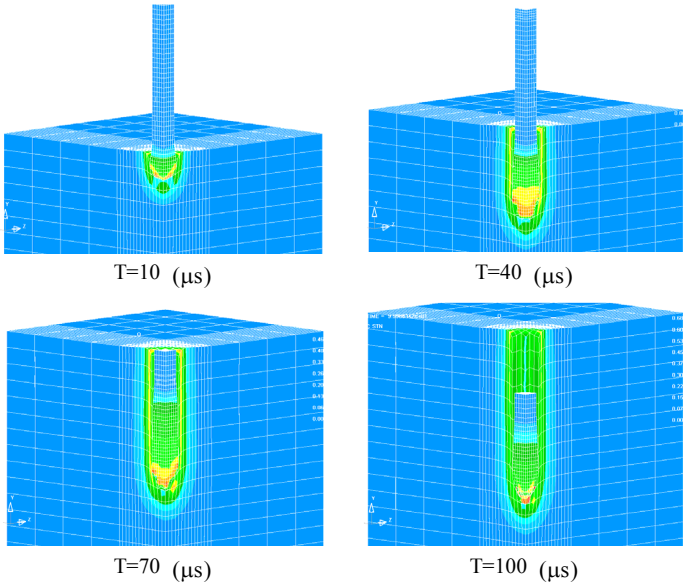

Fig.8. Penetration of Conical Nose-Shape Projectile into the Target Chronologically

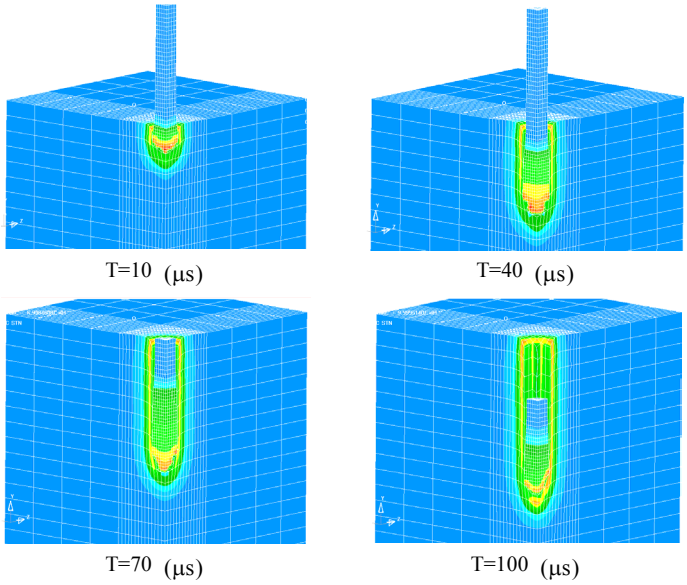

Fig.9. Penetration of Blunt Nose-Shape Projectile into the Target Chronologically

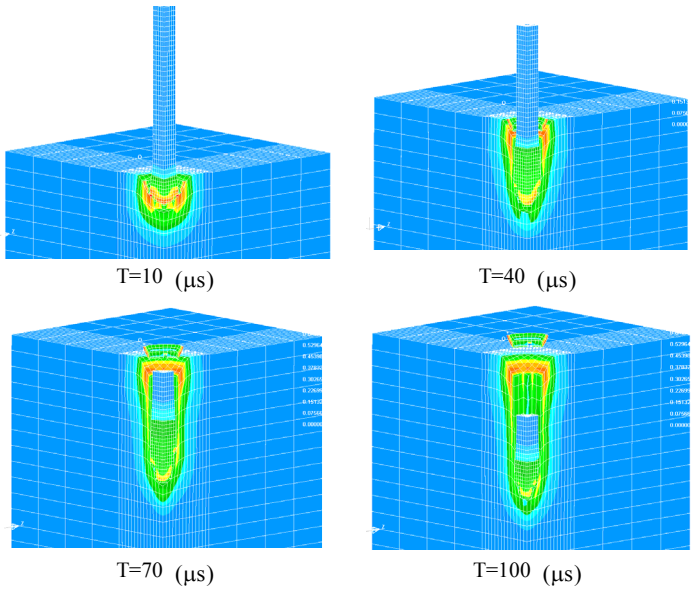

Fig.10. Penetration of T Nose-Shape Projectile into the Target Chronologically

5. Conclusion

In this study effects of nose-shape projectile in penetration to semi-infinite targets is investigated. And the case carried out with two theoretical models: Vahedi and Tate. The results illustrate the point that Vahedi model shows closer agreement with the numerical ones in comparison with Tate model. Also the results emphasis that the projectile nose-shape is effective in final penetration depth. Among these four investigated projectiles, the hemispherical nose-shape projectile has the deepest penetration.

References

(1) Walker J. D, Anderson C. E. The influence of initial nose shape in eroding penetration. *International Journal of Impact Engineering,* Vol 15 (1994), pp. 139-148.
(2) Rosenberg Z., Dekel E. On the role of nose profile in long-rod penetration. *International Journal of Impact Engineering,* Vol. 22 (1999), pp. 551- 557.
(3) Borvik T, Langseth M, Hopperstad O.S, Malo K.A. Perforation of 12 mm thick steel plates by 20 mm diameter projectiles with flat, hemispherical and conical noses Part1: Experimental study. *International Journal of Impact Engineering,* Vol. 27 (2002), pp. 19-35.
(4) Borvik T, Hopperstad O. S, Berstad T, Langseth M. Perforation of 12 mm thick steel plates by 20 mm diameter projectiles with flat, hemispherical and conical noses Part2: Numerical simulations. *International Journal of Impact Engineering,* Vol. 27 (2002), pp. 37-64.
(5) Tate A. A Theory for the deceleration of long rods after impact. *Journal of Mech. Phys. Solids.* Vol. 15 (1967), pp. 387-399.
(6) Ghaseminia A. Vahedi K., The comparison study of long-rod penetration models in semi-infinite targets. *M.S. Thesis, Emam Hossein University.2001*
(7) Mulline S.A, Riegel J.P, Tenenbaum D.A, Erdley D.W. Dynamic plasticity modeling of conical and blunt nosed projectiles and dual layer comparatives study of nose profile role in long-rod penetration. *Paper 152 armor, TACOM Combat Vehicle Survivability Symposium. Gaithenburg, MD. April 15-17.1991.*
(8) Wilkins M.L. Mechanics of penetration and perforation. *International Journal of Engineering Sience,* Vol. 11 (1987), pp. 793- 807.
(9) Hill R. Cavitation and the influence of head-shape in attack of thick targets by non-deforming projectiles. *Journal of Mech. Phys. Solids.* Vol. 28 (1980), pp. 294-263.
(10) Batra R.C. Effect of nose shape and strain hardening on steady state penetration of viscoplastic targets. *In Computational Plasticity, Models, Software and Applications, Pineridge Press, Swansea, U.K. 1987.*
(11) Alekseveevskii V.P. Penetration of arod into a target at high velocity. *Comb. Expl. Shock Waves.* Vol. 2 (1966), pp. 63-66.